Available online at www.sciencedirect.com
SCIENCE DIRECT
Journal of Sound and Vibration 295 (2006) 294–316
JOURNAL OF SOUND AND VIBRATION
www.elsevier.com/locate/jsvi

Thermoelastic buckling and vibration behavior of a functionally graded sandwich beam with constrained viscoelastic core

Rajesh K. Bhangale, N. Ganesan*

Machine Design Section, Department of Mechanical Engineering, Indian Institute of Technology Madras, Chennai 600036, India

Received 5 May 2005; received in revised form 21 December 2005; accepted 14 January 2006
Available online 11 April 2006

Abstract

In this article, buckling and vibration behavior of a functionally graded material (FGM) sandwich beam having constrained viscoelastic layer (VEL) is studied in thermal environment by using finite element formulation. The FGM sandwich beam is assumed to be clamped on both edges. The material properties of FGM are functionally graded in thickness direction according to volume fraction power law distribution. Temperature dependent material properties of FGM stiff layer and shear modulus of viscoelastic layer are considered to carry out buckling and vibration analysis. Numerical studies involving the understanding the effect of power law index, core to stiff layer ratio on the thermal buckling temperature as well as on vibration has been carried out. In addition influence of temperature on natural frequencies and loss factors have been examined for FGM sandwich beam.

1. Introduction

Special composite materials collectively known as functionally graded material (FGM) has been developed due to its excellent mechanical and thermal properties. The concept of FGM was proposed in 1984 by a group of materials scientists, in Sendai, Japan, for thermal barrier or heat shielding properties [1–4]. These types of inhomogeneous composite materials and systems are presently in the forefront of materials research receiving worldwide attention and much research activities have been accelerated. The advantage of using these materials is that they are able to withstand high-temperature gradient environments while maintaining their structural integrity. It possesses properties that vary gradually and continuously with respect to the spatial coordinates in order to achieve a required function. The composition is varied from a ceramic rich surface to metal rich surface with a desired variation of the volume fraction of the two materials in between two surfaces can be easily manufactured [5]. Initially, FGM were designed as thermal barrier materials for aerospace application and fusion reactors. Later on, FGM are developed for military, automotive, biomedical application, semiconductor industry, manufacturing industry and general structural element in thermal environments [6].

*Corresponding author. Tel.: +91 44 22578174; fax: +91 44 2350509.
E-mail addresses: rajesh_phd@iitm.ac.in (R.K. Bhangale), nganesan@iitm.ac.in (N. Ganesan).

0022-460X/$ - see front matter © 2006 Elsevier Ltd. All rights reserved.
doi:10.1016/j.jsv.2006.01.026

Nomenclature

A area of the element in xy plane
E^i, $i = 1,2$ Young's modulus of ith stiff layer
F^{the} element thermal load vector
h thickness of the core layer
h_t heat transfer coefficient, $\text{W/m}^2\,\text{K}$
k thermal conductivity, $\text{W/m}\,\text{K}$
K^e element stiffness matrix
K_g^e element geometric stiffness matrix
l_x, l_y direction cosines in respective directions
M^e element mass matrix
N matrix of shape functions
N_k, $k = 1,2,3,4$ shape functions corresponding to node, k
P_{cr} critical buckling load corresponding to T_b
q heat flux, W/m^2
t_c/t_s ratio of core to stiff layer
t^i, $i = 1,2$ thickness of ith stiff layer
T temperature, °C
T_b buckling temperature
T_k, $k = 1,2,3,4$ temperature at node, k
T_∞ ambient temperature, °C
$w_p, \theta_p, u_p^1, u_p^2$, $p = 1,2$ degrees of freedom at node p
z coordinate measured from the neutral axis of individual layer
α^i, $i = 1,2$ coefficient of thermal expansion of ith stiff layer
$\dot{\delta}^e$ time derivative of δ^e
ΔT^i, $i = 1,2$ temperature above ambient of ith stiff layer
ε^i, γ^c, $i = 1,2$ normal strain in ith stiff layer and shear strain in the core, respectively
ε_0^i, $i = 1,2$ normal strain in middle layer of ith stiff layer
ε^n equal nonlinear strain for each stiff layer
θ' equal bending component of normal strain for each stiff layer
σ^i, τ^c, $i = 1,2$ normal stress in ith stiff layer and shear stress in the core, respectively
σ^{it}, $i = 1,2$ initial normal stress in ith stiff layer
ρ^i, ρ^c, $i = 1,2$ density of ith stiff layer and that of the core

Damping is very important in structures subjected to dynamic loading because it reduces dynamic stress level, increases fatigue life. One of the ways of controlling the noise and vibration in structures is to use a passive damping treatment. The traditional passive control methods for airborne noise include the use of absorbers, barriers, mufflers, silencers, etc. For reducing structure-borne vibration and noise, several methods are available. Something just changing the system's stiffness or mass to alter the resonance frequencies can reduce the unwanted vibration as long as the excitation frequencies do not change. But in the most cases, the vibration needs to be isolated or dissipated by using isolator or damping material. Passive damping as a technology has been dominant in the non-commercial aerospace industry, manufacturing industry since the early 1960s. Advance in the material technology along with newer and more efficient analytical and experimental tools for modeling the dynamic behavior of materials and structures have led to many application such as inlet guide vanes of jet engines, helicopter cabins, exhaust stacks, satellite structures, equipment panels, antenna structures, truss system, space stations, etc. In general, high damping viscoelastic material firmly attached to the surface of the structural member to the augment damping in the system, primarily, by shear deformation. A viscoelastic material exhibits the characteristics of both a viscous fluid and an elastic solid. It combines the two properties namely it returns to its original shape after being stressed, but does it slowly enough to oppose the next cycle of vibrations. There are two methods of treatment of viscoelastic materials namely, free or unconstrained layer treatment and constrained layer treatment. In the case of constrained layer damping treatment, the damping material is sandwiched between the surface of the structure and thin metallic facing. The flexural modulus of the constraining layer is comparable to that of the base structure. During bending, the viscoelastic material is forced to deform in shear due to excessive difference of the moduli between the viscoelastic material, the base structure and the constraining layer. Therefore, a considerable amount of energy is dissipated through shear deformation. Passive damping using sandwich viscoelastic core is one of the ways of suppressing vibration and noise over a wide range of frequencies. These types of sandwich structures find their application as sub-components in spacecraft, aerospace, automobile and missile structures. Analysis of sandwich structures has been of interest for many years [7–12]. Bert [13] gave an introductory review of mathematical models, measures and experimental

techniques. Khatua and Cheung [14,15] presented a finite element formulation for the analysis of multi-layer sandwich beams and plates with soft cores. In their work, they have neglected the normal stress developed in the core and the transverse shear in the stiff layers. Nabi and Ganesan [16] developed a sandwich triangular plate element based on a modified Ahemad approach. Ramesh and Ganesan [17] have analyzed the damping characteristics of a three layered sandwich conical shells. Ramasawamy and Ganesan [18] investigated vibration and damping analysis of fluid filled orthotropic cylindrical shells with constrained viscoelastic damping. They have used the complex eigenvalue approach and have restricted their numerical studies to the first axial mode. Saravanan et al. [19] have analyzed the vibration behavior of multilayer fluid-filled tanks by making use of semi analytical finite element method. Their study concluded that the modal strain energy method improved the computational efficiency when compared to eigenmode analysis. Rao and Nakara [20] carried out analysis of vibration of unsymmetrical sandwich beams and plates with viscoelastic cores. Rao [21] derived the complete set of equations of motion and boundary conditions governing the vibration of sandwich beams using energy approach. Siesmore and Darvennes [22] have considered the effect of compression energy of the core on damping in addition to the conventional approach, which uses only shear deformation of the core for the estimation of damping. Recently, Banerjee [23] has used the dynamic stiffness method for free vibration analysis of three-layer sandwich beams. Ha [24] developed a procedure for exact buckling of sandwich beams and framed structures subjected to arbitrary mechanical loading. The work of Lan et al. [25] presents the thermal buckling of bimodular sandwich beams having thick facings and moderately stiff cores. In recent years, studies on FGM structures in thermal environments are an attractive emerging area in the research community [26–30]. Studies on thermal buckling and free vibration analyses of FGM beam are rare in the literature. Recently, Librescu et al. [31] carried out vibration and stability analysis of thin-walled FGM beams operating in high temperature environment.

From the literature survey on sandwich beam it is visible that buckling and vibration behavior of FGM beam under thermal environment has not been investigated. Hence, the present investigation proposes to investigate the same. Thermal effects considerably affect the buckling and vibration behavior of the FGM structures. For the evaluation of these phenomena in a thermal environment by finite element procedure the prerequisite is the calculation of induced thermal stresses in the structure and then using the evaluated stresses for further analysis. The present finite element formulation is a decoupled thermo mechanical formulation. The temperatures in the sandwich FGM beam domain are evaluated for the given thermal boundary conditions using four-noded beam finite element formulation. For buckling and frequency analyses a two-noded sandwich beam element is used. The estimated temperatures are used for the evaluation of geometric stiffness matrix, which introduces the effect of prestresses into the buckling and frequency eigenvalue problems. The material properties of viscoelastic materials depends significantly on environmental condition such as environment temperature, vibration frequency, pre-load, dynamic load, and environmental humidity. In the present study the dependence of the shear modulus of the viscoelastic core with temperature is considered. The average temperature of the viscoelastic core is used for finding the shear modulus value, which in turn is used to form the element structural stiffness matrix. A parametric study is conducted on viscoelastic sandwich beam with different core to thickness ratios. The effect of the temperature dependence of the shear modulus of the core is considered and compared with the case where the shear modulus is assumed to be constant. In the present study, the variation of FGM material properties with respect to temperature has been accounted and iterative procedure adopted.

2. Analytical model of FGM material properties

FGMs are typically made from a mixture of ceramic and metal or a combination of different metals. Ceramic constituent of the material provides the high-temperature resistance due to its low thermal conductivity. The ductile metal constituent, on the other hand, prevents fracture causes by stresses due to high-temperature gradient in a very short period of time. Consider an FGM sandwich beam as shown in Fig. 1.

In the present analysis, it is assumed that the composition of FGM stiff layer is varied from the top to the bottom surfaces, i.e., the top surface ($Z = -h/2$) of the beam is ceramic-rich, whereas the bottom surface ($Z = h/2$) is metal-rich. In addition material properties are graded throughout the thickness direction

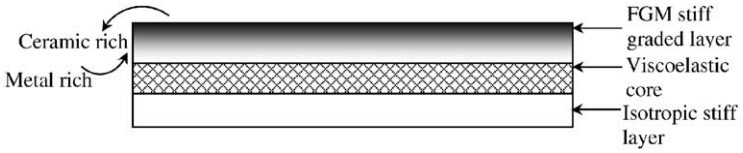

Fig. 1. Configuration of functionally graded sandwich beam having constrained viscoelastic core.

according to volume fraction power law distribution. As FGMs are mainly used in high-temperature environments the constituent materials possess temperature-dependent properties. The properties can be expressed as follows [6]:

$$P = P_0(P_{-1}T^{-1} + 1 + P_1T + P_2T^2 + P_3T^3), \tag{1}$$

where P_0, P_{-1}, P_1, P_2, and P_3 are constants in the cubic fit of the materials property. The materials properties are expressed in this way so that higher order effects of the temperature on the material properties can be readily discernible. Volume fraction is a spatial function whereas the properties of the constituents are functions of temperature. The combination of these functions gives rise to the effective material properties of FGMs and can be expressed by

$$P_{\text{eff}}(T, z) = P_m(T)V_m(z) + P_c(T)(1 - V_m(z)), \tag{2}$$

where P_{eff} is the effective material property of the FGMs, and P_m and P_c are the temperature dependent properties metal and ceramic, respectively. V_m is the volume fraction of the metal constituent of the FGM can be written by

$$V_m = \left(\frac{2z + h}{2h}\right)^n, \quad V_c = 1 - V_m, \tag{3}$$

where volume fraction index n dictates the material variation profile through the beam thickness and may be varied to obtain the optimum distribution of component materials ($0 \leqslant n \leqslant \infty$).

From above equation, the effective Young's modulus E, the Poisson ratio v, mass density ρ and thermal expansion coefficient α of an FGM beam can be written by

$$\begin{aligned}
E_{\text{eff}} &= (E_m - E_c)\left(\frac{2z + h}{2h}\right)^n + E_c,\\
v_{\text{eff}} &= (v_m - v_c)\left(\frac{2z + h}{2h}\right)^n + v_c,\\
\rho_{\text{eff}} &= (\rho_m - \rho_c)\left(\frac{2z + h}{2h}\right)^n + \rho_c,\\
\alpha_{\text{eff}} &= (\alpha_m - \alpha_c)\left(\frac{2z + h}{2h}\right)^n + \alpha_c,\\
k_{\text{eff}} &= (k_m - k_c)\left(\frac{2z + h}{2h}\right)^n + k_c.
\end{aligned} \tag{4}$$

2.1. Finite element formulation for temperature evaluation

The thermal boundary conditions and the relative values of the thermal conductivities of the core and stiff layers influence the temperature distribution in the beam. Temperature in the sandwich beam may vary across the thickness or along the length or both. To capture this effect two-dimensional four-noded rectangular element is used. The steady-state Fourier heat conduction equation in two dimensions without internal heat generation is given by

$$k\left(\frac{\partial^2 T}{\partial x^2} + \frac{\partial^2 T}{\partial y^2}\right) = 0 \tag{5}$$

with the associated boundary conditions

$$l_x \frac{\partial T}{\partial x} + l_y \frac{\partial T}{\partial y} = h_t(T - T_\infty) + q \quad \text{on surface } S_1,$$

$$T = T_0 \quad \text{on surface } S_2.$$

The differential equation (5) along with the associated boundary conditions can be turned into equivalent variational expression, given by

$$I = \frac{1}{2}\int\int_A \begin{pmatrix} \frac{\partial T}{\partial x} \\ \frac{\partial T}{\partial y} \end{pmatrix} K \begin{pmatrix} \frac{\partial T}{\partial x} & \frac{\partial T}{\partial y} \end{pmatrix} \mathrm{d}A + \frac{1}{2}\int_{S_1} qT \,\mathrm{d}s + \frac{1}{2}\int_{S_1} h_t(T^2 - 2TT_\infty)\,\mathrm{d}s. \tag{6}$$

The temperature T can be expressed in terms of nodal temperatures T_k and shape functions N_k as $T = \sum_{k=1}^{4} N_k T_k$. Substituting the value of T in Eq. (6) then minimizing the expression with respect to nodal temperatures T_k, the following elemental matrix equation can be obtained

$$K_1^e T^e + K_2^e T^e = P_1^e + P_2^e, \tag{7}$$

where

$$K_1^e = \int_A B_t^{\mathrm{T}} K B_t t \,\mathrm{d}x\,\mathrm{d}y,$$

$$K_2^e = h\int_{S_1} N_t^{\mathrm{T}} N_t \,\mathrm{d}S,$$

$$P_1^e = h_t T_\infty \int_{S_1} N_t^{\mathrm{T}} \,\mathrm{d}S,$$

$$P_2^e = q\int_{S_1} N_t^{\mathrm{T}} \,\mathrm{d}S,$$

$$N_t = (N_1 N_2 N_3 N_4), \quad T^e = (T_1 T_2 T_3 T_4)^{\mathrm{T}}.$$

2.2. Finite element formulation for structural analysis

The FGM sandwich beam element is developed based on the displacement field proposed by Khatua and Cheung [14]. The assumptions made for formulating sandwich beam element are the following:

1. The core is soft and viscoelastic having a shear modulus $G = (G^{*c} + i\eta G^{*c})$ and cannot carry any normal stress.
2. Shear stress in the stiff layers is neglected.
3. All the points at any cross section of the beam will have same transverse displacement and bending slope.
4. The plane section is assumed to remain plane for each core layer.

The deformed shape of any cross section of sandwich beam under loading can be expressed in terms of transverse displacement of the cross section (w), the bending slope at that cross section (θ) and the axial displacements of top and bottom layers (u^1, u^2), as shown in Fig. 2(a). Two-noded FGM sandwich beam finite element is shown in Fig. 2(b). The degrees of freedom associated with each node will be the four above-mentioned parameters.

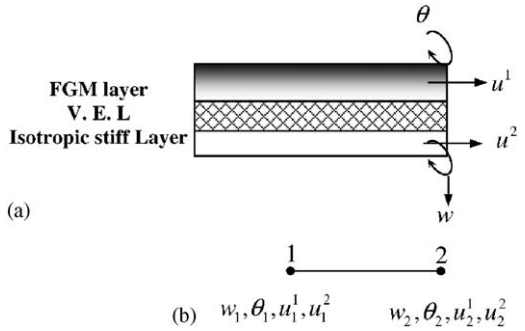

Fig. 2. FGM sandwich beam element.

The stress–strain relations for a sandwich beam continuum under thermal environment can be written by [25]

$$\begin{pmatrix} \sigma^i \\ \tau^c \end{pmatrix} = \begin{pmatrix} E^i & 0 \\ 0 & G^{*c} \end{pmatrix} \begin{pmatrix} \varepsilon^i - \alpha^i \Delta T^i \\ \gamma^c \end{pmatrix}, \quad i = 1, 2. \tag{8}$$

Assuming that each stiff layer will bend about its own neutral axis the total strain energy can be written by

$$U_1 = \int (\sigma^1 \varepsilon^1 \, \mathrm{d}v^1 + \sigma^2 \varepsilon^2 \, \mathrm{d}v^2 + \tau^c \gamma^c \, \mathrm{d}v^c). \tag{9}$$

By substituting $\varepsilon^1 = \varepsilon_0^1 + z\theta'$ and $\varepsilon^2 = \varepsilon_0^2 + z\theta'$ the above expression and performing integration in the thickness and width directions U_1 can be written by

$$U_1 = \int_x \varepsilon^{*\mathrm{T}} (D\varepsilon^* - D^* \varepsilon^{th}) \, \mathrm{d}x \tag{10}$$

$\varepsilon^{*\mathrm{T}} = (\theta' \varepsilon_0^1 \gamma^c \theta' \varepsilon_0^2)^{\mathrm{T}}$ and $\varepsilon^{th\mathrm{T}} = (0 \alpha_{\mathrm{eff}}^1 \Delta T^1 0 0 \alpha^2 \Delta T^2)^{\mathrm{T}}$. Superscripts 1, 2, and c indicate the quantities related to top, bottom, and core layers, respectively. Making use of shape functions in the strain displacement relations given in Appendix, the strain array ε^* can be written in terms of nodal displacement δ^e as $B\delta^e$. Substituting the expression for ε^* in Eq. (10) and minimizing the total strain energy with respect to δ^e the following equation can be obtained:

$$\begin{aligned} \int_x B^{\mathrm{T}} DB \, \mathrm{d}x (\delta^e) &= \int_x B^{\mathrm{T}} D^* \varepsilon^{th} \, \mathrm{d}x, \\ K^e (\delta^e) &= F^{\mathrm{the}}, \end{aligned} \tag{11}$$

where $K^e = \int_x B^{\mathrm{T}} DB \, \mathrm{d}x$ is the element stiffness matrix, $F^{\mathrm{the}} = \int_x B^{\mathrm{T}} D^* \varepsilon^{th} \, \mathrm{d}x$ is the element thermal load vector and $\delta^e = (w_1, \theta_1, u_1^1, u_1^2, w_2, \theta_2, u_2^1, u_2^2)^{\mathrm{T}}$.

The expression for the geometric stiffness matrix can be obtained from the expression for work done by the membrane forces during small transverse displacements of the beam.

The expression for this work is given by

$$U_2 = \frac{1}{2} \int \sigma^{1t} \varepsilon^n \, \mathrm{d}v^1 + \frac{1}{2} \int \sigma^{2t} \varepsilon^n \, \mathrm{d}v^2, \tag{12}$$

$$U_2 = \frac{1}{2} \int_x \varepsilon^{*n} \sigma^t \varepsilon^{*n\mathrm{T}} \, \mathrm{d}x,$$

where $\varepsilon^{*n} = (\sqrt{\varepsilon^n}, \sqrt{\varepsilon^n})$. ε^{*n} can be written as $B_g\delta^e$ and substituting this value in Eq. (12) the expression for U_2 becomes

$$U_2 = \frac{1}{2}\delta^{e\mathrm{T}} K_g^e \delta^e,$$

where $K_g^e = \int_x B_g^{\mathrm{T}} \sigma^t B_g \, \mathrm{d}x$ is the element geometric stiffness matrix.

The expression for total kinetic energy in the sandwich beam element continuum can be written by

$$\begin{aligned} \mathrm{KE} = 0.5 &\int (\rho_{\mathrm{eff}}^1 \, \mathrm{d}v^1 + \rho^2 \, \mathrm{d}v^2 + \rho^c \, \mathrm{d}v^c)\dot{w}^2 \\ &+ 0.5 \int (\rho_{\mathrm{eff}}^1 \, \mathrm{d}v^1 + 0.5\rho^c \, \mathrm{d}v^c)(\dot{u}^1)^2 \\ &+ 0.5 \int (\rho^2 \, \mathrm{d}v^2 + 0.5\rho^c \, \mathrm{d}v^c)(\dot{u}^2)^2. \end{aligned} \tag{13}$$

After performing the integrations in the thickness and width directions, and making use of shape functions in Eq. (13) the kinetic energy can be written by

$$\mathrm{KE} = \frac{1}{2}\dot{\delta}^{e\mathrm{T}} M^e \dot{\delta}^e,$$

where $M^e = \int_x N^{\mathrm{T}} P N \, \mathrm{d}x$ is the element mass matrix.

The expressions for D^*, B_g, σ^t are given in Appendix. The expressions for B, D, and P can be realized in the paper by Khatua and Cheung [14]. Expressions for K_1^e, K_2^e, P_1^e, and P_2^e are given in Rao [31].

3. Results and discussion

This section presents the frequency, damping and buckling behaviors of sandwich beam under thermal environment. The computer code developed for the analysis has been validated based on the data available in the literature. Thermal stresses are estimated in the beam and buckling and vibration analyses are carried out. Present study deals with FGM sandwich beam with clamped–clamped boundary condition. The dimensions of the beam are given below.

$$\text{Thickness of each stiff layer} = t_s = t^1 = t^2 = 3\,\mathrm{mm},$$

$$\text{Length of the beam } (l) = 0.6\,\mathrm{m}.$$

3.1. Validation

As there is no open literature available on vibration and buckling behavior of FGM sandwich beam it is felt that result can be compared for isotropic material sandwich beam with that of buckling of isotropic sandwich beam under mechanical loading by incorporating power law index as $n = 0.0$, in the present computer code developed for FGM sandwich beam. For this purpose a clamped–clamped beam subjected to uniform temperature is analyzed as it leads to constant compressive stresses. In order to validate the buckling code, fixed–fixed sandwich beam of length 0.5 m with thickness of each stiff layer 3 mm and having a 3 mm thick core was considered. The beam is subjected to constant temperature so that normal stress is constant through out the length of the beam. The material properties of the beam are similar to those specified in Fig. 3. Based on the buckling temperature the compressive stresses and corresponding critical buckling load can be evaluated. The analytical expression for the critical buckling load of sandwich beams can be found in a paper by Ha [24]. Table 1 compares the finite element solution and analytical value of critical buckling load and the results obtained by the present code match well with the results of literature.

In addition damping of viscoelastic sandwich beam without temperature are evaluated and compared with the value in the existing literature. The computer code developed is validated for its damping behavior for the dimensions given in Ref. [21]. The dimensions of the beam along with the material properties of the layers are given in Fig. 3.

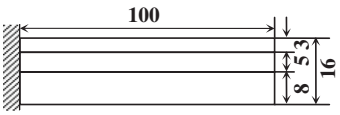

$E^1 = E^2 = 20.6e10N/m^2$, $G^{*c} = 0.98e10N/m^2$
$\rho^1 = \rho^2 = 7850Kg/m^2$, $\rho^c = 2600Kg/m^2$, $\eta = 0.1$

Fig. 3. Sandwich beam configuration for validation purpose [21].

Table 1
Comparison of buckling load

Description	Finite element solution			From the formula given by Ha [24]
	10 elements	20 elements	30 elements	
T_b (°C)	142.55	139.16	138.55	—
P_{cr} (KN)	31.009	30.272	30.139	30.034

Table 2
Comparison of frequency and loss factor

Description	Finite element solution			Exact values by Rao [21]
	10 elements	20 elements	40 elements	
f (Hz)	1307.04	1305.77	1305.53	1309
η	0.006935	0.006898	0.006898	0.006965

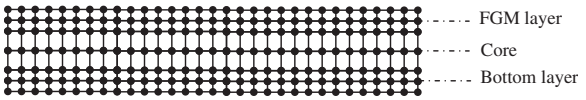

Fig. 4. Finite element mesh for layer wise temperature evaluation.

Table 2 compares the first mode resonant frequency (f) of the above beam and the loss factor (η) with exact values given by Rao [21]. There is a good agreement between the exact values and finite element solution.

3.2. Thermal analysis

Thermal environments will influence the buckling and frequency behavior of a structure. This effect can be accounted for by the estimation of thermally induced prestresses. In the present study, layer-wise temperatures in the sandwich beam are calculated using the four-noded rectangular elements. Fig. 4 shows the finite element mesh for temperature evaluation. Each layer is meshed with two rectangular elements in thickness direction and 30 elements are used in the length direction. Three different thermal boundary conditions (TBC1, TBC2 and TBC3) are considered for analysis as shown in Fig. 5.

The further analysis has been carried out for the following cases of temperature boundary condition.

(1) TBC1–FGM sandwich beam heated at one edge.
(2) TBC2–FGM sandwich beam at the top surface.

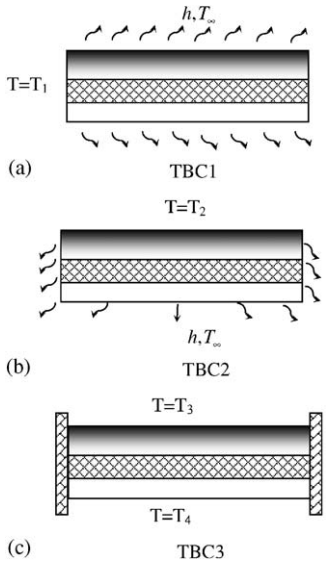

Fig. 5. Temperature boundary conditions.

(3) TBC3–FGM sandwich beam insulated at two edges and specified temperature at top and bottom such that temperature gradient is developed.

The relevant elemental matrices indicated in Eq. (7) are assembled by applying the desired boundary condition. The nodal temperatures are obtained by solving the following equation:

$$K_1^G T^G + K_2^G T^G = P_1^G \tag{14}$$

with the superscript G indicating corresponding global matrices. The nodal temperatures on the middle line of each layer are extracted and these are considered to be approximate layer temperatures for prestress estimation.

The temperature distributions in the sandwich beam for the two different cases of thermal boundary conditions are shown in Fig. 6. The graphs are drawn for a specified temperature 160 °C for the given boundary condition. Fig. 6(a) shows temperature variation along the length of the beam with thermal boundary condition TBC1. The temperature falls down from the specified temperature (160 °C) at right end following a second-order curve as indicated in Fig. 6(a). No appreciable variation of temperature in thickness direction of the beam can be observed with thermal boundary condition TBC1. Fig. 6(b) shows the variation of temperature across the thickness of the beam with thermal boundary condition TBC2. The temperature at any cross section along the length of the beam remains almost constant in the top layer (160 °C), drops linearly in viscoelastic core and remains almost constant in the bottom layer. Temperature along the length of the beam is a constant with thermal boundary condition TBC3. Moreover similar temperature pattern is observed in case of TBC2.

3.3. Static thermal buckling analysis of functionally graded sandwich beam having constrained viscoelastic layer and clamped–clamped boundary conditions

Having validated the present model to a certain extent in present study an attempt has been made to study the thermal buckling behavior of FGM viscoelastic sandwich beam made up of mixture of metal and ceramic. The viscoelastic core material used is EC2216. The evaluation of thermal buckling temperature is based on classical stability equation involving the structural stiffness matrix, K_{nR}^G, and initial stiffness matrix, K_{gn}^G.

$$[K_{nR}^G] + \lambda[K_{gn}^G] = 0. \tag{15}$$

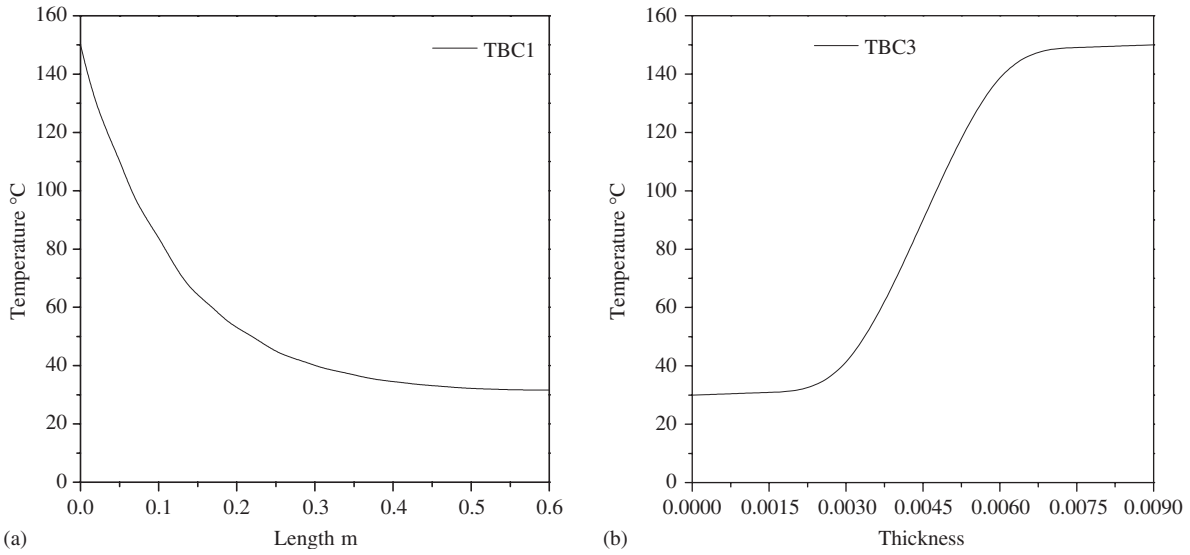

Fig. 6. (a) Temperature variation along the length of the sandwich beam for TBC1 and (b) temperature variation across the thickness of the sandwich beam for TBC3.

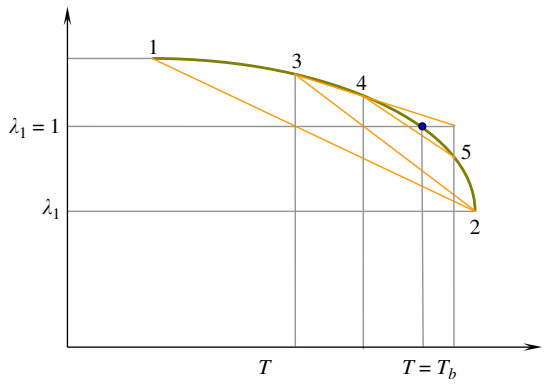

Fig. 7. Iterative algorithm for finding buckling temperatures when G^* and material properties are temperature dependent.

The buckling eigenvalues and buckling mode shapes are computed using the simultaneous iteration technique. A typical configuration of the functionally graded viscoelastic beam is assumed to be ceramic rich on the top surface and metal rich on the bottom surface. The FGM structure material properties are dependent on temperature. In addition complex shear modulus of the viscoelastic core G^* is also a function of temperature. The thermal buckling study has been carried out by accounting the variation of material properties with respect to temperature. As the problem becomes nonlinear, iterative procedure has been adopted. The overall procedure followed for the determination of the converged thermal buckling temperature is best understood from the flow chart presented in Fig. 7.

First to start with, assume a particular temperature, and temperature dependent material properties evaluate λ. The procedure starts with two initial guesses, namely points 1 and 2 as shown in Fig. 7. The temperature T_l corresponding to $\lambda_1 = 1$, is found by linear interpolation or extrapolation using the points 1 and 2 and the improved guess 3 is found by reevaluating the value of λ_1 at the temperature T_l. Now 2 and 3 will be new guess points for the next iteration. The procedure is repeated by using the last two guesses till the two guesses converge to the buckling temperature T_b and $\lambda_1 = 1$.

Thermal buckling analysis of FGM beam is carried out in two steps. First, the heat conduction equation is solved for temperature distribution for different temperature boundary condition across the thickness of the shell. Variation of temperature along the length of the shell is also calculated. The thermal material property is dependent on temperature and hence a converged temperature distribution is obtained. Based on the converged temperature distribution the mechanical and thermal properties are evaluated.

An exercise is taken up to illustrate the necessity of considering temperature dependent material properties of FGM structures and complex shear modulus of viscoelastic core. Following two cases are considered.

Case A: Temperature distribution obtained is based on the thermal properties assumed at room temperature. Thermal buckling temperature is computed based on the material properties at room temperature. The complex shear modulus value for EC2216 is 344.8 MPa at room temperature.

Case B: Thermal buckling temperatures are computed based on the procedure illustrated in flow chart (see Fig. 7). It accounts for temperature dependent material properties of structure and temperature dependent complex shear modulus of EC2216.

The results are presented in Tables 3 and 4 for FGM sandwich beam viz., SUS304-Al2O3 for temperature boundary conditions TBC2 and TBC3. The critical buckling temperature estimated according to procedure of Case A is higher when compared to the buckling temperature computed using the procedure of Case B. Thus buckling temperatures obtained as per Case B procedure are more conservative. From Tables 3 and 4, it is concluded that the thermal buckling strength has been reduced while taking into temperature dependent material properties. For temperature boundary condition TBC1 thermal buckling results are reported in Table 5. It is seen that thermal buckling strength is higher in case of TBC1. In this case critical temperature is higher than the operating temperature limit of VEL material (EC2216) for higher core thickness to stiff later ratios. Hence, buckling and vibrations studies not reported here. But it is visible from Table 5 that effect of temperature dependent material properties is felt more at higher buckling temperature and higher power law index approaching to homogeneous ceramic side. Tables 3 and 4 show the converge lowest buckling temperature for SUS304-Al_2O_3 FGM sandwich beam having EC2216 has VEL core for the TBC2 and TBC3 of temperature boundary condition for various power law index. Here power law index $n = 0.0$ corresponds to an isotropic shell with properties corresponds to that of metal (SUS304) and $n = 1000.0$ corresponds to FGM beam purely of ceramic material (Al_2O_3). The power law indexes value n other than two extreme values govern the distribution of properties of metal and ceramic mixture in FGM stiff layer. Variation of the composition of metal and ceramic is linear for power law index $n = 1.0$. From Tables 3 and 4, it is found that as the value of power law index n increases the critical buckling temperature increases as it approaching towards the homogeneous ceramic composition for all t_c/t_s ratios. Such trend is observed because of coefficient of thermal expansion of ceramic is lower than metal. In addition as the thickness ratio of core to the stiff layer increases the thermal buckling strength of FGM sandwich beam increases. Further it is seen that TBC2 at slight higher

Table 3
Converged lowest critical buckling temperature in °C for SUS304-Al_2O_3 FGM sandwich beam having EC2216 has a VEL core and TBC2 type of boundary condition for various power law index

Power law index n	Case A			Case B		
	$G^{*c} = C$			$G^{*c} = f(t)$		
	$t_c/t_s = 1$	$t_c/t_s = 2$	$t_c/t_s = 3$	$t_c/t_s = 1$	$t_c/t_s = 2$	$t_c/t_s = 3$
0.0	91.90	147.58	213.84	83.69	122.46	165.35
0.2	94.36	151.75	219.79	85.60	125.20	168.89
0.5	98.19	158.44	229.60	88.65	129.82	175.11
1.0	104.39	169.60	246.33	93.66	137.76	186.16
2.0	114.51	188.38	275.05	101.96	151.37	205.60
5.0	128.11	214.55	315.99	113.15	170.43	233.56
10.0	132.00	222.29	328.31	116.36	176.06	241.98
1000.0	132.41	223.11	329.63	116.72	176.65	242.88

Table 4
Converged lowest critical buckling temperature in °C for SUS304-Al_2O_3 FGM sandwich beam having EC2216 has a VEL core and TBC3 type of boundary condition for various power law index

Power law index n	Case A			Case B		
	$G^{*c} = C$			$G^{*c} = f(t)$		
	$t_c/t_s = 1$	$t_c/t_s = 2$	$t_c/t_s = 3$	$t_c/t_s = 1$	$t_c/t_s = 2$	$t_c/t_s = 3$
0.0	90.08	139.79	196.00	84.01	118.67	153.04
0.2	92.49	143.74	201.52	85.93	121.24	156.04
0.5	96.22	150.09	210.65	88.96	125.53	161.23
1.0	102.27	160.69	226.26	93.91	132.80	170.36
2.0	112.19	178.93	253.35	101.98	145.09	188.03
5.0	125.57	203.89	292.72	112.72	161.99	213.72
10.0	129.43	211.43	304.79	115.82	166.91	221.52
1000.0	129.84	212.23	306.08	116.15	167.43	222.35

Table 5
Converged lowest critical buckling temperature in °C for SUS304-Al_2O_3 FGM sandwich beam having EC2216 has a VEL core and TBC1 type of boundary condition for various power law indexes

Power law index n	Case A			Case B		
	$G^{*c} = C$			$G^{*c} = f(t)$		
	$t_c/t_s = 1$	$t_c/t_s = 2$	$t_c/t_s = 3$	$t_c/t_s = 1$	$t_c/t_s = 2$	$t_c/t_s = 3$
0.0	305.28	—	—	296.56	—	—
0.2	334.79	—	—	324.63	—	—
0.5	380.15	—	—	368.61	—	—
1.0	488.86	—	—	460.75	—	—
2.0	725.56	—	—	580.25	—	—
5.0	1130.98	—	—	798.84	—	—
10.0	1531.25	—	—	1020.25	—	—
1000.0	1548.58	—	—	1021.58	—	—

buckling strength as compared to TBC3. It is also found from the results when the shear modulus is higher the core thickness strongly influences buckling temperature. In contrast if the shear modulus is low the core thickness does not influence buckling temperature much. Similar trend in mechanical critical buckling load can be observed when the formula given by Ha [24] is used.

3.4. Effect of temperature on the free vibration frequency and modal loss factor of FGM sandwich beam and clamped–clamped boundary conditions

To understand the behavior of the natural frequency variation with respect to temperature, studies have been carried out on SUS304-Al_2O_3 FGM sandwich beam. The temperature on the outer surface is varied in steps of suitable increments and the highest temperature for the study is limited to the lowest thermal buckling temperature for the beam configuration and FGM composition (or power law index n). Based on the converged temperature distribution, the thermal load vector, total initial stresses and hence the geometric stiffness matrix is computed. This initial stiffness matrix is added to the FGM sandwich beam stiffness (real) matrix and along with mass matrix leads to the following eigenvalue problem.

$$[K_R^G + K_g^G]\phi - \omega^2 M^G \phi = 0 \tag{16}$$

The modal loss factor for jth mode ϕ_j can be found at any given temperature from the following equation:

$$\eta_j = \frac{\phi_j^{\mathrm{T}} K_R^G \phi_j}{\phi_j^{\mathrm{T}} (K_I^G + K_g^G) \phi_j}, \tag{17}$$

where η_j is the loss factor for the jth mode and K_R^G, K_I^G are the real and imaginary parts of global stiffness matrix K^G, respectively. $[K_g^G]$ is evaluated at the given temperature. In present case in order to see the effect of temperature dependent shear modulus and material properties on frequency and loss factors following cases are considered for similar temperature boundary condition. To start with, study has been carried out by considering the shear modulus of VEL core and material properties at room temperature. The shear modulus, loss factor values of viscoelastic core materials namely EC2216 at 30 °C and at 100 Hz are 620.5 MPa, 0.3 [12].

Fig. 8 shows the variation of frequency and modal loss factor of a sandwich beam with temperature for core (EC2216) thickness for power law index $n = 0$, 1.0 and 1000.0, respectively. Fig. 8 shows the variation of frequency and loss factor with temperature for first four modes of the sandwich beam with different power law index as a parameter with thermal boundary condition TBC3. The shear modulus of the core is assumed to remain constant with respect to temperature and properties of FGM layer also at room temperature. Fig. 8(a), (c) and (d) shows that natural frequencies increases with increase in power law exponent n, as it approaching towards the homogeneous ceramic composition. This trend has been expected because of Young's modulus of ceramic is higher than that of metal. Further it is seen that mode 1 it is the mode corresponding to the lowest thermal buckling temperature. Mode 1 is associated with reasonably high bending strain energy. As the temperature increases fall in natural frequencies gradually and continuously. There is no appreciable drop in frequency is observed with respect to temperature for all modes. This behavior is noticed for all n. Further the characteristic variation of the natural frequency with respect to temperature depends on the mode numbers. The buckling temperatures of the higher modes are higher. Similarly for higher modes the partial fall in frequency for the initial increase in temperature is to be noted. This is because the buckling temperature for higher modes is higher. In addition there may be the dominating influence of the bending strain energy and the effect of temperature rise is less. Thus it is clear that the effect of temperature is felt more for the modes corresponding to the lowest thermal buckling temperature. The loss factor for the first mode of the beam gradually increases with respect to temperature reaching a very high value when temperature approaches the buckling temperature for any given thickness of the beam. This trend is expected because the value of the denominator in the expression for modal loss factor decreases as the temperature increases due to decrease in the total stiffness of the sandwich beam. As the power law index n increases there is slight increase in modal loss factor. Further study has been carried out for $t_c/t_s = 2.0$ and $t_c/t_s = 3.0$. Similar discussion hold good for $t_c/t_s = 2.0$ and 3.0. Figs. 9 and 10 show that as increase in the core thickness results in increase in modal loss factors appreciably.

Further study has been carried out by accounting temperature dependent shear modulus of the core and material properties of FGM stiff layer. The temperature dependent plots of G^{*c} and η for the EC2216 are given in Ref. [10]. A curve is fitted to the plots given in Ref. [10] such that values of G^{*c} and η can be obtained from it at any temperature in the operating range of temperatures. These curves are used for studying the buckling, frequency and loss factor variations with temperature when temperature dependent properties of the core are used. Fig. 11 shows the variation of natural frequency and loss factor for FGM sandwich beam for $n = 0.0$, 1.0, 1000.0, respectively, with EC2216 as a core material for TBC3 type of temperature boundary condition. It can be seen from Figs. 11(a) and 8(a) that first mode frequency variation is almost coincident for both the cases i.e. with constant shear modulus case and temperature dependent shear modulus case of the core. Remaining higher modes deviate appreciably when temperature dependent shear modulus is used. The effect of temperature dependent shear modulus and FGM properties causing frequencies comes down to zero at earliest buckling temperature as compared to previous one. This effect is felt more for higher t_c/t_s ratios. Here one can observe a fall in frequency appreciably for higher modes with respect to temperature as compared to Fig. 8. Figs. 11(b), (d) and (f) show the variation of loss factor with temperature for $n = 0.0$, 1.0, 1000.0, respectively, for $t_c/t_s = 1.0$. From Figs. 11 and 13 it is seen that loss factor pattern is much different when temperature dependent shear modulus is used. It is seen from Figs. 11 and 13 that all mode shape behavior appears as a curve type. The first mode increases continuously and attains a higher value near

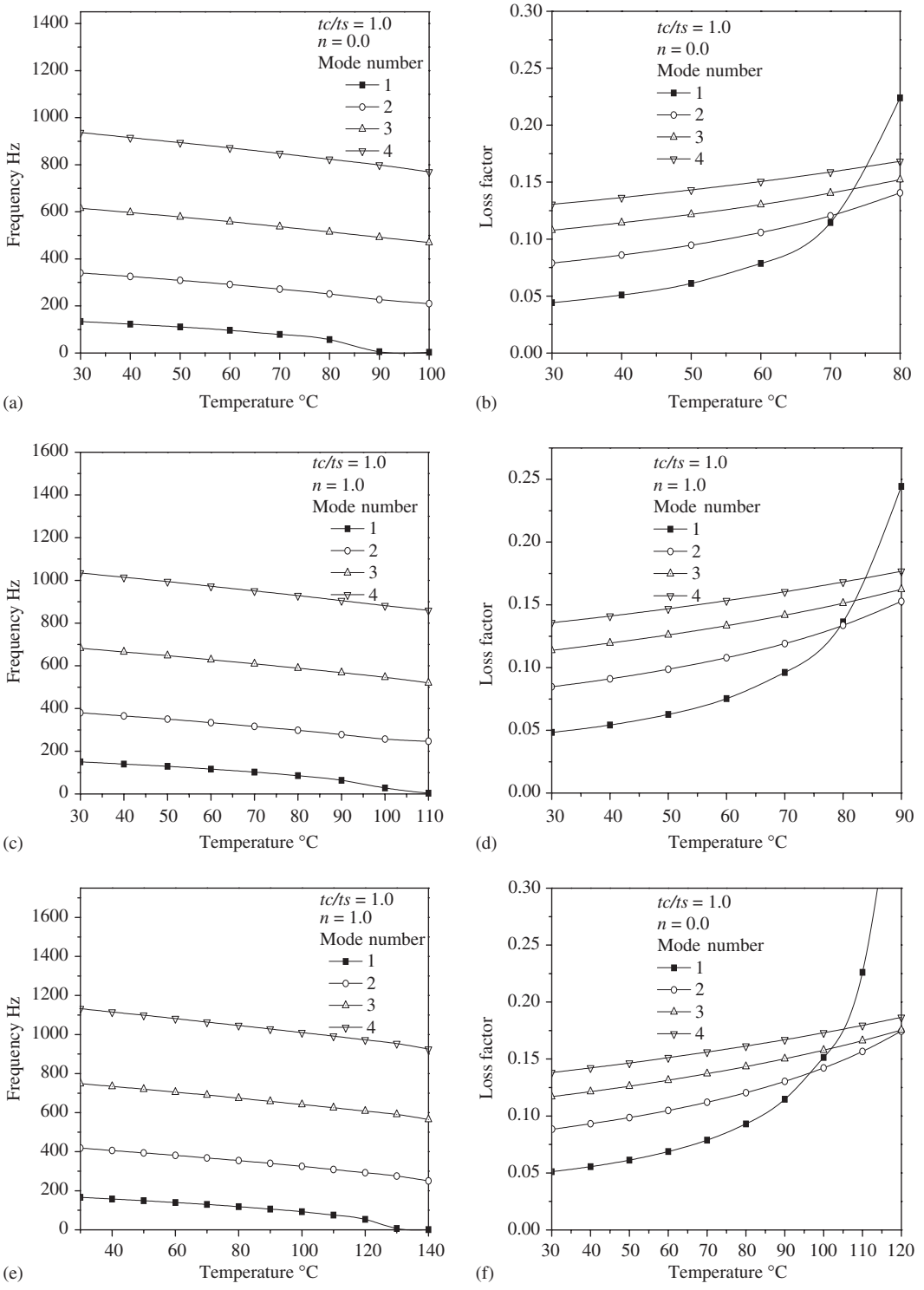

Fig. 8. Variation of frequency and loss factors for VEL sandwich SUS304-Al_2O_3 FGM beam temperature independent shear modulus for core EC2216 ($t_c/t_s = 1.0$).

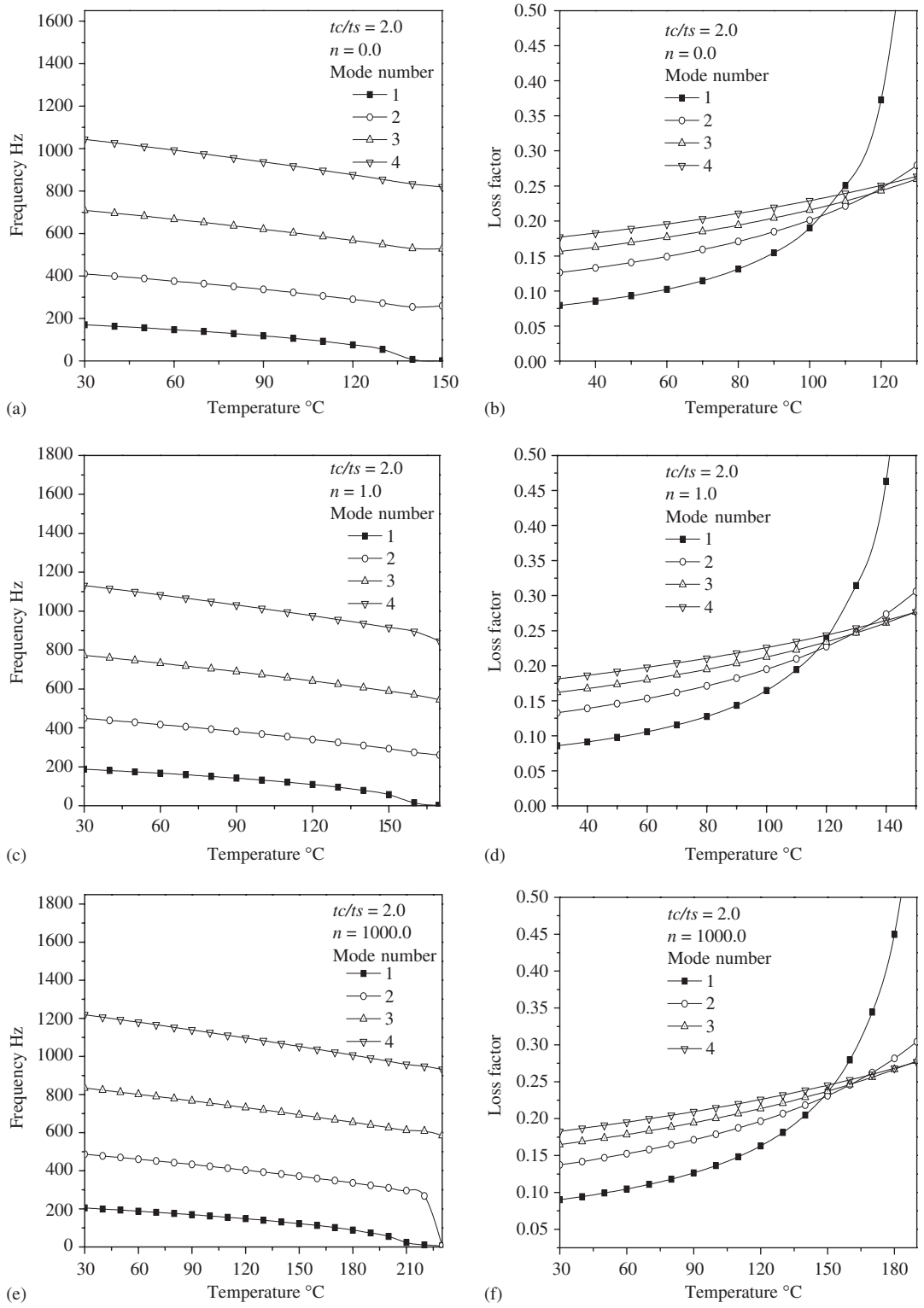

Fig. 9. Variation of frequency and loss factors for VEL sandwich SUS304-Al_2O_3 FGM beam temperature independent shear modulus for core EC2216 ($t_c/t_s = 2.0$).

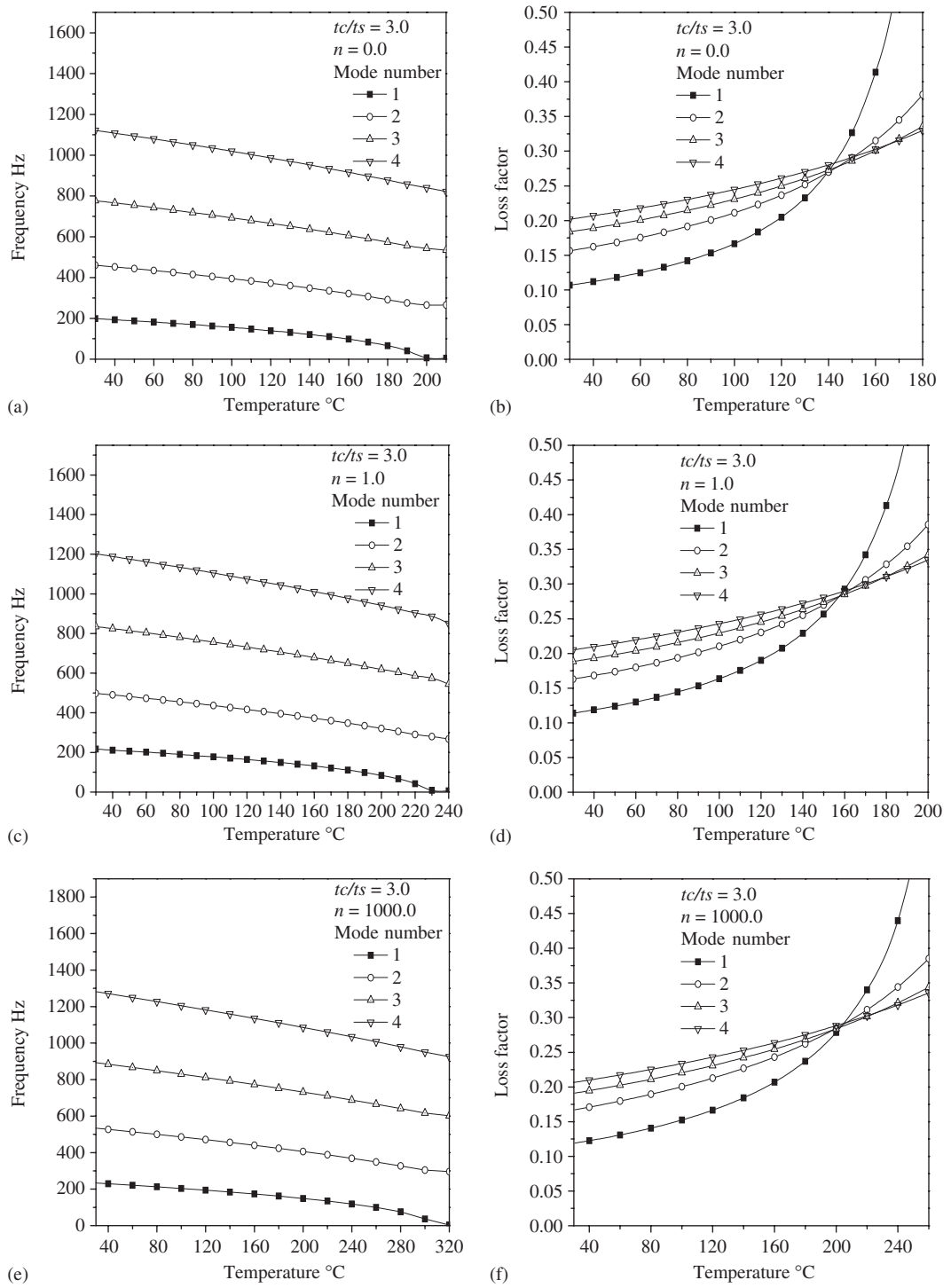

Fig. 10. Variation of frequency and loss factors for VEL sandwich SUS304-Al_2O_3 FGM beam temperature independent shear modulus for core EC2216 ($t_c/t_s = 3.0$).

buckling temperature. Loss factors of remaining higher modes deviate appreciably when temperature dependent shear modulus is used. Here modal loss factor increase upto certain temperature then decreases and again starts increasing near to the critical buckling temperature. Similar behavior has been observed for other

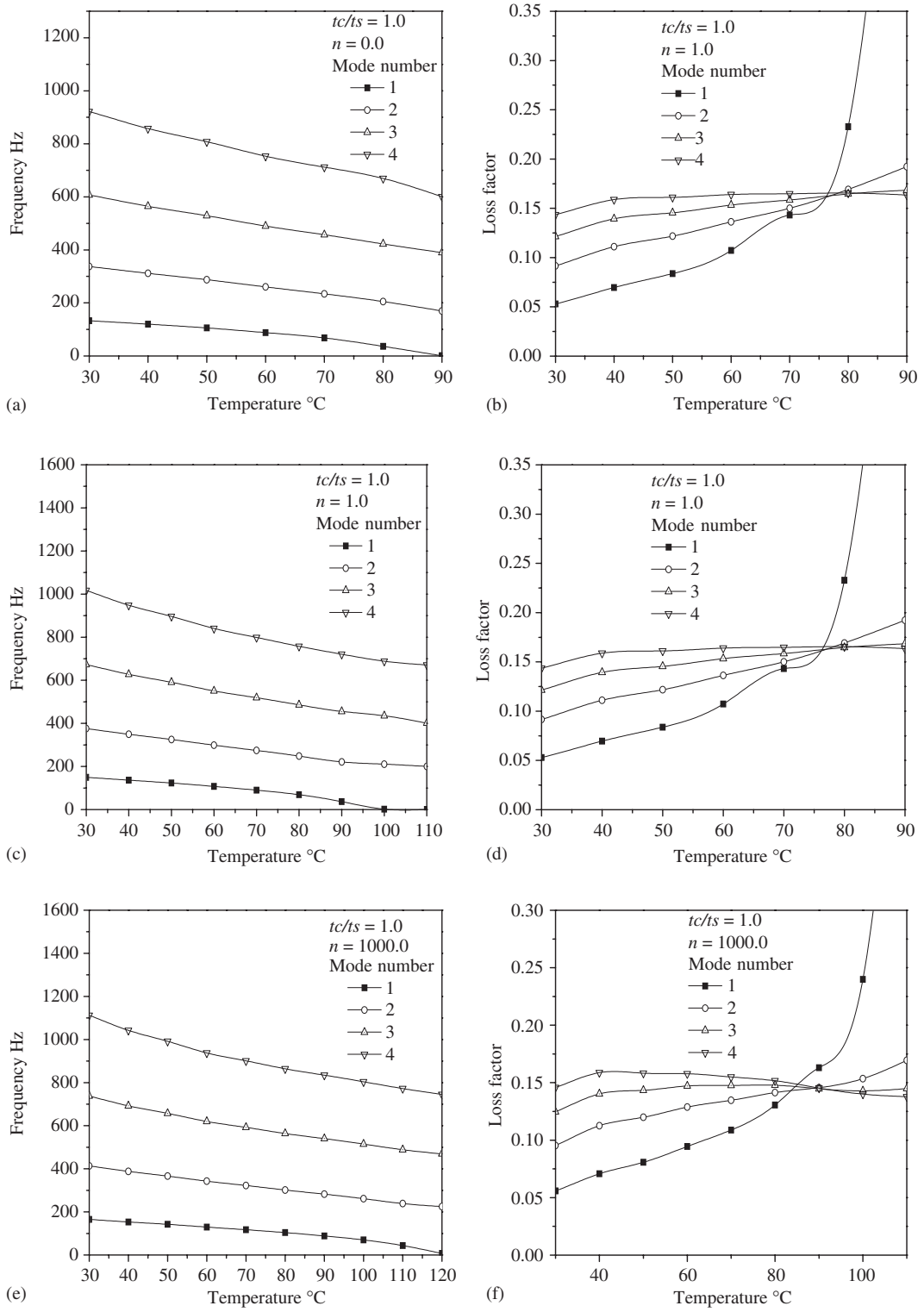

Fig. 11. Variation of frequency and loss factors for VEL sandwich SUS304-Al_2O_3 FGM beam with temperature dependent shear modulus for core EC2216 ($t_c/t_s = 1.0$).

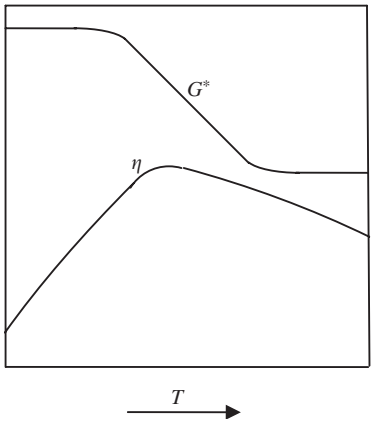

Fig. 12. Variation of G^* and η with temperature for a viscoelastic solid with temperature.

power law index $n = 1.0$ and 1000.0 shown in Figs. 11(d) and (f). This fact can be ascribed by looking the characteristics curve of EC2216 for η as shown in Fig. 12 [12]. It is seen that the value of η for a viscoelastic material increases initially with temperature and reaches a peak value and there after reduces.

Same discussion holds good for other type of t_c/t_s ratios and power law index n shown in Figs. 13 and 14. Increase in the core thickness results in increased modal loss factor of the FGM sandwich beam significantly. By increasing in core thickness magnitude of frequency are increases marginally. The modal loss factors increases up to a certain temperature and then start decreases. As the power law index n increases the modal loss factor also increases marginally. So it is concluded that consideration of temperature dependent shear modulus causes the buckling strength reduces causing an early drop in frequency with respect to temperature. So in order to do accurate analysis it is preferable to consider temperature dependent material properties.

4. Conclusion

A thermal buckling and vibration analysis of functionally graded sandwich beam having constrained viscoelastic layer has been carried out by finite element method. The FGM beam is graded in the thickness direction and a simple power law index will govern the metal–ceramic constituents profile across the thickness. The FGM sandwich beam is assumed as a multilayered beam with each layer to possess homogeneous isotropic properties; this model forms the basis for evaluating the material constitutive matrix. The thermal material property is dependent on temperature and hence a converged temperature distribution is obtained. Based on the converged temperature distribution the mechanical properties and thermal property are evaluated. The shear modulus of the viscoelastic core is also temperature dependent. The converged temperature distribution will be the thermal loading on the beam. Thermal buckling temperature is evaluated until convergence is obtained. Effect of temperature dependent material properties of FGM layer as well as temperature dependent shear modulus on the buckling and vibration behavior has been investigated for EC2216 as a core materials. The following conclusions are arrived from present study.

1. The magnitude of the lowest buckling temperature of FGM sandwich beam greatly depends on the composition of the metal–ceramic constituent. The thermal buckling temperature depends on the coefficient of thermal expansion. Materials with lower coefficient of thermal expansion will have high thermal buckling temperature.
2. The critical buckling temperature for a FGM sandwich beam increases as the power law index n increases.
3. Thermal buckling strength of the FGM sandwich beam has been reduced when the temperature-dependent properties are taken into consideration.
4. As expected, by increasing the ratio of the core to stiff layer thermal buckling temperature increases.

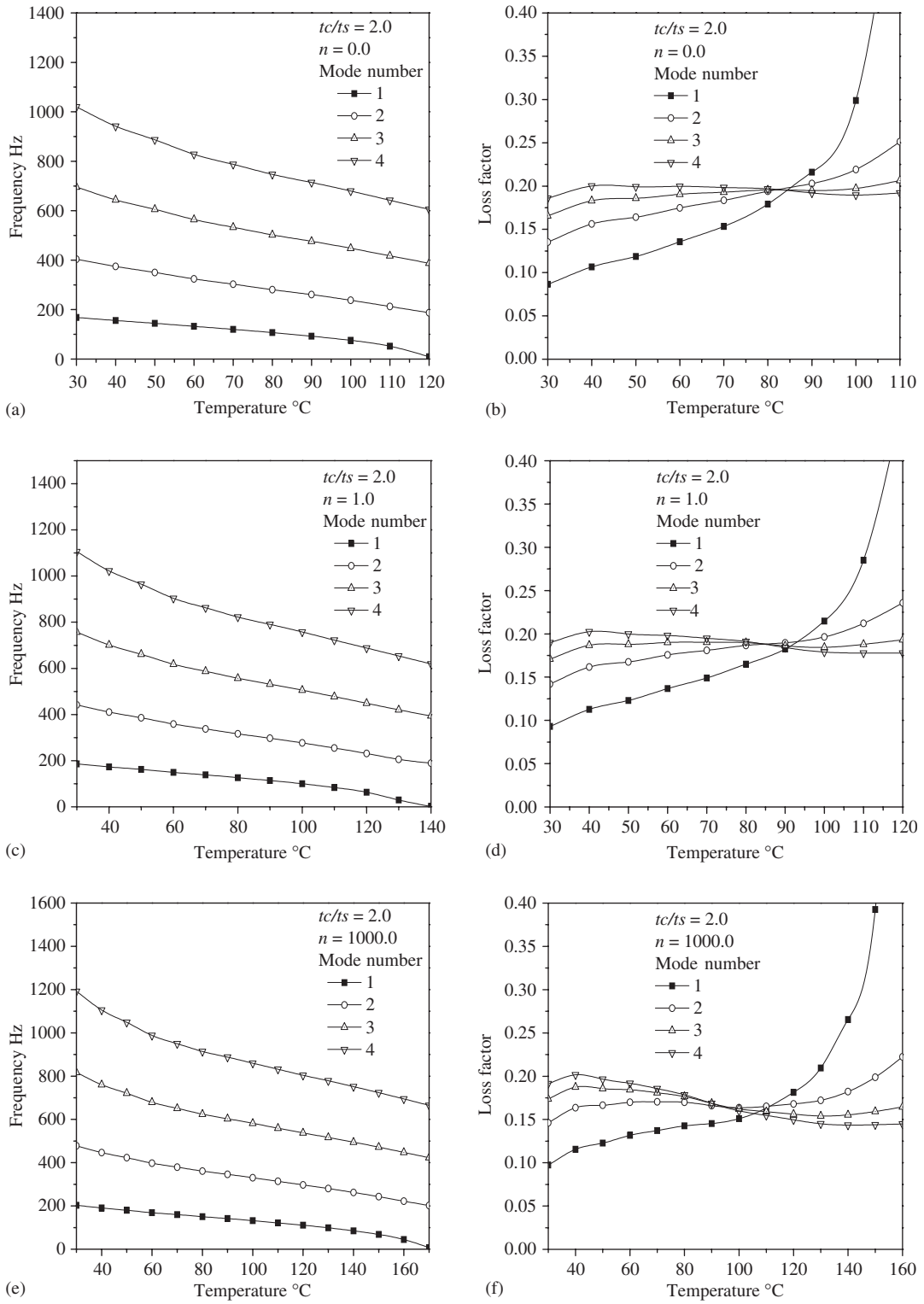

Fig. 13. Variation of frequency and loss factors for VEL sandwich SUS304-Al_2O_3 FGM beam with temperature dependent shear modulus for core EC2216 ($t_c/t_s = 2.0$).

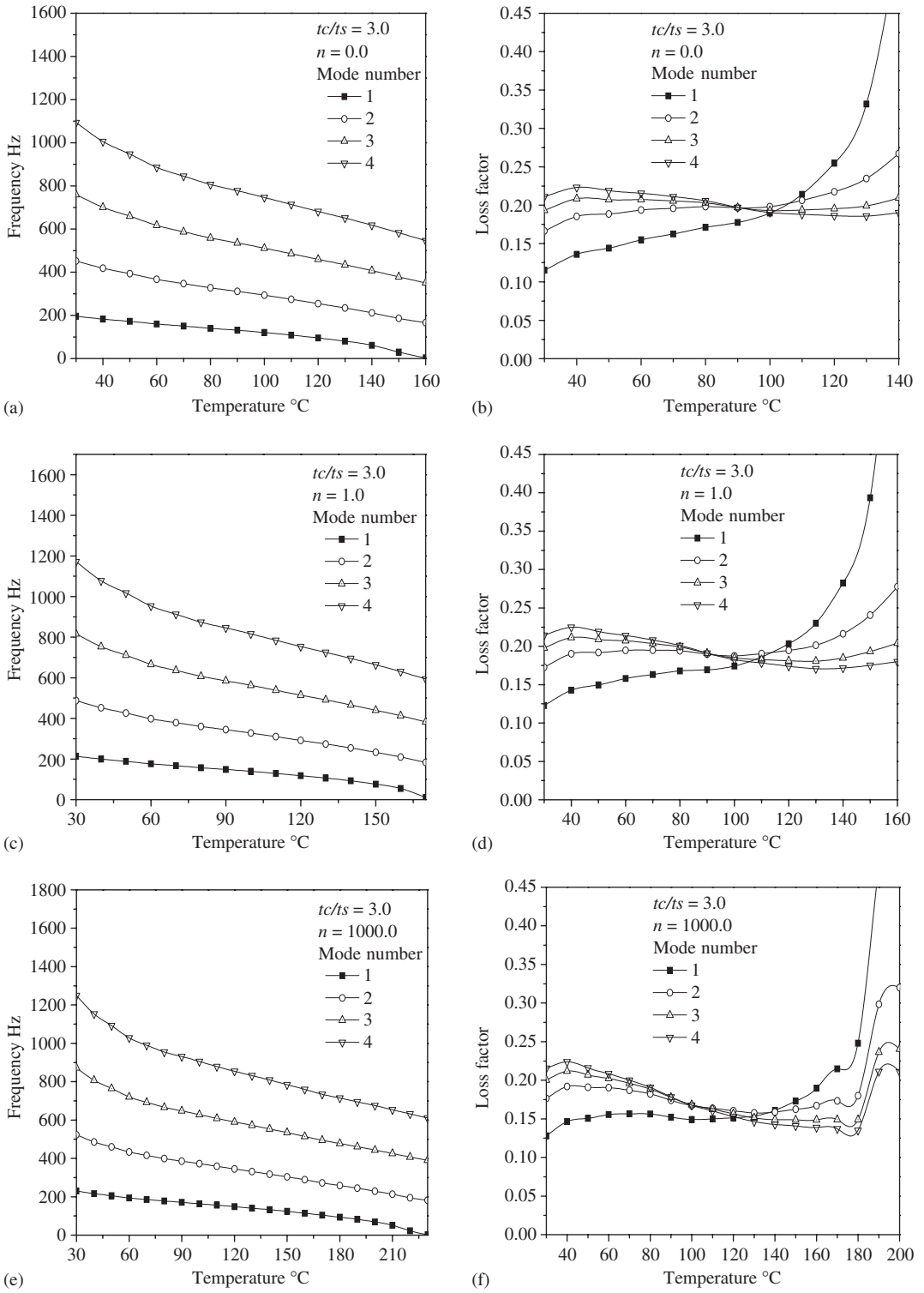

Fig. 14. Variation of frequency and loss factors for VEL sandwich SUS304-Al_2O_3 FGM beam with temperature dependent shear modulus for core EC2216 ($t_c/t_s = 3.0$).

5. Natural frequency of the FGM sandwich beam increases as power law index n increases when approaching to homogeneous ceramic side.
6. The effect of temperature on the natural frequency of FGM sandwich beam is to reduce the natural frequency with increase in temperature.
7. The effect of temperature dependent shear modulus of the viscoelastic core is felt predominantly at higher modes. The loss factor pattern is much different when temperature dependent shear modulus is used. Effects of temperature on loss factors are more pronounced for material EC2216 whose shear modulus varies more dramatically investigated over the temperature range.
8. For the buckling temperature range considered in the present study η was increasing with temperature. In addition real stiffness of the system is falling with temperature. Hence in general the damping was increasing with temperature. It is felt that this conclusion may not hold good for the range of temperature where η decreases with temperature.

Appendix

Strain displacement relations

The strain terms in the array of generalized strains ε^* are related to the displacements as follows:

$$\theta' = \frac{\mathrm{d}^2 w}{\mathrm{d}x^2},$$

$$\varepsilon_0^i = \frac{\mathrm{d}u^i}{\mathrm{d}x}, \quad i = 1, 2,$$

$$\gamma^c = \frac{C}{h}\left[\frac{u^2 - u^1}{C} + \frac{\mathrm{d}w}{\mathrm{d}x}\right] \quad \text{where } C = h + 0.5(t^1 + t^2),$$

$$\varepsilon^n = \left(\frac{\mathrm{d}w}{\mathrm{d}x}\right)^2,$$

$$[D] = \begin{bmatrix} [D_{b1}] & [D_{c1}] & & & \\ [D_{c1}] & [D_{p1}] & & 0 & \\ & & [D_{\text{core}}] & & \\ & 0 & & [D_{b2}] & [D_{c2}] \\ & & & [D_{c2}] & [D_{p2}] \end{bmatrix},$$

$$[D_{bi}] = \sum_{i=1}^{\text{sublay}} \frac{E_{\text{eff}} b[(t_{i+1})^3 - (t_i)^3]}{3},$$

$$[D_{ci}] = \sum_{i=1}^{\text{sublay}} \frac{E_{\text{eff}} b[(t_{i+1})^2 - (t_i)^2]}{2},$$

$$[D_{pi}] = \sum_{i=1}^{n\,\text{sublay}} E_{\text{eff}} b[(t_{i+1}) - (t_i)],$$

$$[D_{\text{core}}] = \sum_{i=1}^{n\,\text{sublay}} [(h_{i+1}^c - h_i^c)],$$

$$D^* = \begin{pmatrix} 0 & & & & \\ & bE^1_{\text{eff}}t^1 & & & \\ & & 0 & & \\ & & & bE^2t^2 & \\ & & & & 0 \end{pmatrix}, \quad \sigma^t = \begin{pmatrix} bt^1\sigma^{1t} & 0 \\ 0 & bt^2\sigma^{2t} \end{pmatrix},$$

$$B_g = \begin{pmatrix} N_{11,x} & N_{12,x} & 0 & 0 & N_{21,x} & N_{22,x} & 0 & 0 \\ N_{11,x} & N_{12,x} & 0 & 0 & N_{21,x} & N_{22,x} & 0 & 0 \end{pmatrix}.$$

N_{ij}, $i = 1, 2$ and $j = 1, 2$ are the shape functions [14] suffix x indicates the derivative with respect to x.

References

[1] M. Koizumi, FGM activities in Japan, *Composites* 28 (Part B) (1997) 1–4.
[2] M. Koizumi, M. Niino, Overview of FGM research activities in Japan, *Material Research Society Bulletin* 20 (1995) 19–21.
[3] K. Ichikawa, *Functionally Graded Materials in the 21st Century. A Workshop on Trends and Forecasts*, Kluwer, Boston, 2001.
[4] B.V. Sankar, J.T. Tzeng, Thermal stress in functionally graded beams, *AIAA Journal* 40 (6) (2002) 1228–1232.
[5] S. Suresh, A. Mortensen, *Fundamentals of Functionally Graded Materials*, IOM communications, London, 1998.
[6] J.N. Reddy, C.D. Chin, Thermomechanical analysis of functionally graded cylinders and plates, *Journal Thermal Stresses* 21 (1998) 593–626.
[7] B.J. Lazan, *Damping of Materials and Members in Structural Mechanics*, Pergamon Press, Oxford, 1968.
[8] F.H. Chu, B.P. Wang, Experimental determination of damping in materials and structures, in: P.J. Torvik (Ed.), *Damping Application for Vibration Control, ASME Winter Annual Meeting*, Chicago, 1982. pp. 113–122.
[9] D. Ross, E.M. Kervin, E.E. Ungar, Damping of the plate flexural vibration by means of viscoelastic laminate, *Structural Damping, ASME,* New York, 1959 (Section II).
[10] E.M. Kervin, Damping of flexural waves by a constrained viscoelastic layer, *Journal for Acoustical Society of America* 31 (1959) 952–962.
[11] K.M. Ahmad, Static and dynamic analysis of sandwich structures by the method of finite element, *Journal of Sound and Vibration* 18 (1) (1971) 75–91.
[12] A.D. Nashif, D.I.G. Jones, J.P. Henderson, *Vibration Damping*, Wiley, New York, 1985.
[13] C.W. Bert, Material damping: an introductory review of mathematical models, measures and experimental techniques, *Journal of Sound and Vibration* 29 (1973) 129–153.
[14] T.P. Khatua, Y.K. Cheung, Bending and vibration of multi layer beams and plates, *International Journal for Numerical Methods in Engineering* 6 (1973) 11–24.
[15] T.P. Khatua, Y.K. Cheung, Stability analysis of multilayer sandwich structures, *AIAA Journal* 2 (9) (1973) 1233–1234.
[16] M.S. Nabi, N. Ganesan, Sandwich triangular plate element based on a modified Ahmed approach, *Journal of Sound and Vibration* 161 (3) (1993) 545–547.
[17] T.C. Ramesh, N. Ganesan, Finite element analysis of conical shells with a constrained viscoelastic layer, *Journal of Sound and Vibration* 171 (1992) 577–601.
[18] R. Ramasawamy, N. Ganesan, Vibration and damping analysis of fluid filled orthotropic cylindrical shells with constrained viscoelastic damping, *Computers and Structures* 70 (3) (1998) 363–376.
[19] C. Saravanan, N. Ganesan, V. Ramamurti, Vibration and damping analysis of multi layered fluid filled shells with constrained viscoelastic damping using modal strain energy method, *Computers and Structures* 75 (2000) 395–417.
[20] Y.V.K.S. Rao, B.C. Nakara, Vibrations of unsymmetrical sandwich beams and plates with viscoelastic cores, *Journal of Sound and Vibration* 34 (3) (1974) 309–326.
[21] D.K. Rao, Frequency and loss factors of sandwich beams with various boundary conditions, *Journal of Mechanical Engineering Science* 20 (5) (1978) 271–282.
[22] C.L. Siesmore, C.M. Darvennes, Transverse vibration of elastic–viscoelastic–elastic sandwich beams: compression experimental and analytical study, *Journal of Sound and Vibration* 252 (1) (2002) 155–167.
[23] J.R. Banerjee, Free vibration of sandwich beams using dynamic stiffness method, *Computers and Structures* 81 (2003) 1915–1922.
[24] K.H. Ha, Exact analysis of bending and overall buckling of sandwich beam systems, *Computers and Structures* 45 (1) (1992) 31–40.
[25] T. Lan, P.D. Lin, L.W. Chen, Thermal buckling of bimodular sandwich beams, *Composite Structures* 25 (1993) 345–352.
[26] G.N. Praveen, C.D. Chin, J.N. Reddy, Thermoelastic analysis of functionally graded ceramic-metal cylinder, *Journal of Engineering Mechanics* 125 (1999) 1259–1267.
[27] R. Javaheri, M.R. Eslami, Thermal buckling of functionally graded plates based on higher order theory, *Journal of Thermal Stresses* 25 (2002) 603–625.
[28] R.K. Bhangale, N. Ganesan, Thermal buckling of functionally graded beam, *Proceedings of Third International Conference on Theoretical Applied and Computational Mechanics*, IIT, Kharagpur, 27–30 December 2004, pp. 274–277.

[29] R.K. Bhangale, N. Ganesan, A linear theromoelastic buckling behaviour of functionally graded hemispherical shells with cut-out at apex, *International Journal of Structural Stability and Dynamics* 5 (2005) 185–215.
[30] R.K. Bhangale, N. Ganesan, Linear theromoelastic buckling and free vibration behaviour of functionally graded truncated conical shells, *Journal of Sound and Vibration* (2005) 185–215.
[31] L. Librescu, S.Y. Oh, O. Song, Thin-walled beams made of functionally graded materials and operating in a high temperature environment: vibration and stability, *Journal of Thermal Stresses* 28 (2005) 649–712.